Nanomed Res J 7(1):73-82, Winter 2022

RESEARCH ARTICLE

Preparation and characterization of bovine serum albumin nanocarrier conjugated to exosome to sustained release of 5-flurouracil: Release and antitumoral evaluation

Ghazaleh Rahimi[1], Maryam Saeidifar[1,*], Monireh Ganjali[1], Esmaeel Salahi[2]

[1] *Nanotechnology and Advanced Materials Department, Materials and Energy Research Center, Karaj, Iran*

[2] *Ceramic Department, Materials and Energy Research Center, Karaj, Iran*

ARTICLE INFO

Article History:
Received 02 October 2021
Accepted 20 December 2021
Published 01 January 2022

Keywords:
Albumin
Nanoparticle
Cancer
Exosome
Release Mechanism

ABSTRACT

One of the new strategies for improving of chemotherapy in cancer treatment is the use of nanocarriers for sustained release of anticancer drugs. The present study aims to investigate the bovine serum albumin nanoparticles (BSANP) with exosomes (Exo) for prolonged release of 5-Flurouracil (5FU) as an anticancer drug model. 5FU with Exo was loaded to BSANP (5FU.Exo@BSANP) and the system was characterized by FTIR, AFM and FESEM. Furthermore, 5FU.Exo and 5FU@BSANP were prepared and characterized to compare their release behavior with that of 5FU.Exo@BSANP. The binding properties examined via FTIR confirmed the formation of the above-mentioned systems. FESEM analysis of BSANP and 5FU.Exo@BSANP showed the spherical morphology with the average particle size 313±60 nm and 403±64 nm, respectively, while, 5FU.Exo had a cylindrical morphology with average particle size in width 200±36 nm. AFM results demonstrated the reduction of roughness in 5FU.Exo@BSANP. In addition, the release behavior indicated that sustained release of 5FU occurred when it was loaded to nanocarriers. However, the release of 5FU from 5FU.Exo@BSANP at pH 7.4 was slower than in the other systems. Furthermore, the kinetic model of all systems was followed by Korsmeyer-peppas with Fickian diffusion while 5FU.Exo@BSANP at pH 5.5 was zero order kinetic model. Moreover, MTT assay onto 4T1 cancer cell lines explored the significant cytotoxicity of 5FU.Exo@BSANP. Thus, the designed nanocarrier of Exo@BSANP is a promising system for sustained release of 5FU.

How to cite this article
Rahimi Gh., Saeidifar M., Ganjali M., Salahi E. Preparation and characterization of bovine serum albumin nanocarrier conjugated to exosome to sustained release of 5-flurouracil: Release and antitumoral evaluation . Nanomed Res J, 2022; 7(1): 73-82. DOI: 10.22034/nmrj.2022.01.007

INTRODUCTION

Despite the achievements in cancer treatment, it causes still human death worldwide. Chemotherapy is the most frequently manner for cancer treatment that causes the systematic toxic and adverse side effects [1]. In addition, chemotherapy reduces the efficacy of anticancer drugs due to fast metabolism of drug [2]. To overcome the mentioned problems, researchers are looking for the new pharmaceuticals and improvement efficacy of current anticancer drugs [3]. During the last two decades, nanotechnology have been employed to introduce an appropriate nanocarrier for encapsulation of anticancer drugs that reduces the toxicity, increases the therapeutic effects, prolongs the circulation time in the blood, and protects the drugs until reaching the target [1,4,5]. The nanomaterials should have biocompatibility, high drug-binding capacity, bioactivity and stability properties in biomedical applications [6]. One of the best choice for this application is polymeric nanoparticles that provides the above properties [7,8]. Among the biopolymers as the nanocarriers, natural origin compounds such as polysaccharides, proteins, lipids can be applied in the form of drug vehicles for

* Corresponding Author Email: *saeidifar@merc.ac.ir*

cancer treatment [2,9,10]. In particular, albumins such as bovine serum albumin (BSA) and human serum albumin (HSA) are the promising candidate for sustained release and delivery of anticancer agents [11,12]. Furthermore, exosomes (Exo) with the low toxicity, small size, natural molecular transport properties, and good biocompatibility can be play a significant role in designing novel drug delivery systems [13,14]. Exosomes are nano extracellular vesicles secreted by cells that carry nucleic acids, proteins, lipids and other biological molecules. The exosomes due to endogenetic and heterogenetic properties have unique advantages in medicine compared to synthetic carriers [15,16]. Also, the previous achievements, realized that exosomes as a carrier caused the drugs keep their activity and release the without toxicity [17–19].

In the other hand, 5-Flurouracil (5FU) is one of the anticancer drugs for colon cancer treatment [20]. The limitation of 5FU administration such as rapid metabolism, short half-life and cytotoxicity in the body is being dissolved using many nano-sized carriers, including lipids, hydrogels, dextran and nanomaterials to improve its therapeutic efficacy and reduce its side effects [12,20,22,23].

In this study, the combination of two biocompatible polymer of bovine serum albumin nanoparticles and exosomes was employed to design a nanocarrier and to study sustain release of 5FU chosen as an anticancer model drug. Further, the synthesized nanocarrier systems of 5FU conjugated Exo (5FU.Exo), 5FU loaded BSANP (5FU@BSANP) and 5FU.Exo@BSANP were characterized by FTIR, AFM and FESEM. In addition, the release behavior and release mechanism were analyzed. Furthermore, the cytotoxicity of nanocarrier systems was performed on 4T1 breast cancer cell lines. The aim of this research is the reduce side effects, longer shelf life, and enhance the effectiveness of 5FU.

EXPERIMENTAL SECTION

Materials

Bovine serum albumin (BSA), Phosphate Buffer Saline (PBS), 1-Ethyl-3-(3-Dimethylaminopropyl) Carbodiimide (EDC), penicillin, streptomycin and trypsin-EDTA and dialysis bag (12 kDa) were purchased from Sigma-Aldrich, USA, Ethanol (95%) and HCl (37%) were obtained from Merck, Germany. Exosome (24.3 mM) was prepared according to previous reports [19]. 5-Fluorouracil (5FU, 50 mg/ml) and sodium chloride (0.9%, normal saline) were received from Ebewe Co., Austria and Samen Co., Iran, respectively. RPMI1640, 3-(4,5-dimethylthialzol-a-yl)-2,5-diphenyltetrazolium bromide (MTT), fetal bovine serum (FBS) were purchased from GIBCO, USA. 4T1 breast cancer cell lines were obtained from the cell bank of Pasteur institute in Tehran, Iran. Deionized water was used in all of the experiments and the other reagents and solvents were analytical grad and used as received.

Methods

Fourier Transform Infrared Spectroscopy (FTIR) analysis was recorded to investigate molecular binding by Vector33 model, Bruker, USA spectrometer (KBr tablet and the scan rang of 400-40,000 cm^{-1}). DLS analysis was performed by Zetasizer HS C1330–3000 model, Malvern, UK, to determine size distribution and surface charge of colloidal solutions. The morphology of particles was obtained by field emission scanning electron microscope (FESEM) of Mira 3-XMU, TESCAN, Czech Republic. The surface morphology and particle distribution were recorded by atomic force microscopy (AFM), South Korea's Park Systems Corporation. The UV-Vis spectroscopy was used for detection of drug release and monitored by spectrometer of T80 + model, TG instruments, UK. pH measurements of Metrohm pH-meter, model 826 pH mobile, Switzerland; Digital balance (0.1 mg accuracy) of XS 204 model, Mettler-Toledo, Australia; magnetic stirrer, Wisestir, South Korea; ultrasonic bath Instrument, H6SW, Swiss; and centrifuge (15000 rpm) of R 320/320 Hettich® Universal, Germany were utilized in all of the experiments.

Preparation of BSANP

The synthesis of BSANPs was followed by desolvation method with optimal conditions [9,24]. Briefly, 50 mg/ml of BSA solution was prepared and 8 ml of ethanol as separator (0.54 ml/min rate) was added to BSA solution which was first stirred at 200 rpm. The addition 4 ml of ethanol caused the clear solution of BSA became turbid which indicated a BSA structural change. At this time, to prevent agglomeration, the stirring was done at 400 rpm. Then, 5 mg/ml of EDC as cross-linker was added to the above suspension for stabilization of the created structure. To purification of EDC and excess BSA, the suspension was centrifuged (11,000 rpm for 10 min) and redispersed in deionized water

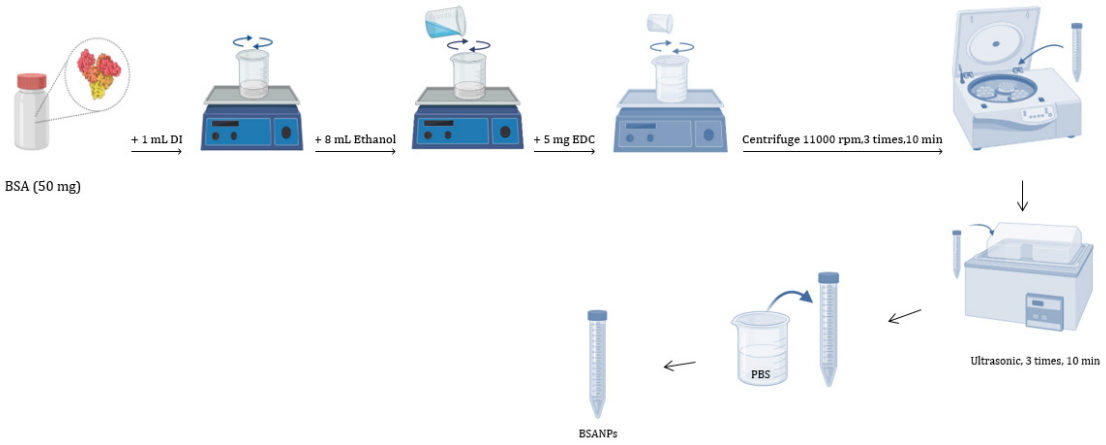

Scheme 1. Schematic of BSANP synthesis

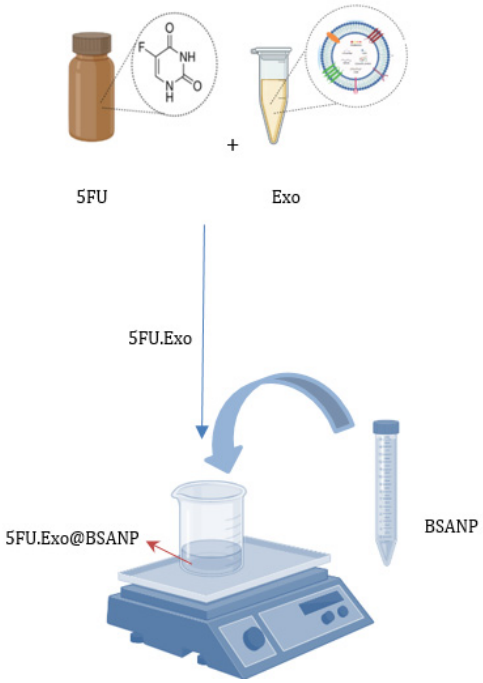

Scheme 2. Preparation protocol of 5FU.Exo@BSANP

under ultrasonic for 5 min (three times). Finally, the sediment of BSANPs (47.6 mg) was dispersed in 10 ml PBS and stored at 4°C in dark. Scheme 1 displays the protocol of BSANP synthesis.

Drug loading experiment

5-Flurouracil (5FU) was separately loaded on three nanocarrier of Exosome (Exo), bovine serum albumin nanoparticles (BSANP), and Exo with BSANP (Exo@BSANP). For this purpose, 60 mL from 5FU (50 mg/ml) were added to the prepared nanocarrier as follows:

1) 1.91 ml of PBS and 32.9 mL from exosome solution (24.3 mM); **2**) 940 mL of PBS and 1 mL from BSANP (4.67 mg/ml) dispersed by ultrasonic without temperature for 5 min; and **3**) 5FU added to 940 mL of PBS containing 32.9 mL from Exo (24.3 mM) and stirred slowly (100 rpm at ambient temperature) for 1 h and then 1 mL of BSANP (4.67 mg/ml) added to the above solution (Scheme 2).

Finally, the total volume of each system was 2 mL. The suspensions were stirred (100 rpm) at room temperature for 24 h in protection from light. After that, 2 mL of the suspension was transferred to a dialysis bag and used for release studies.

Determination of drug concentration

UV-Vis spectrum of 5FU was recorded and wavelength of maximum peak (l_{max}) was selected for other studies. Various concentrations of 5FU, [C], were prepared (0-1.375 mg/mL) with the absorbance (A) recorded at l_{max}. The standard diagram of A versus [C] was plotted whereby a linear trend line and its equation were obtained by excel software as A=m[C], where m is the slope of plot [25]. Accordingly, the absorbance of 5FU at l_{max} was recorded and unknown concentration of drug was calculated by the standard equation.

Determination of drug loading percentage

Drug loading percentage (%DL) is weight proportion of entrapped drug relative to nanocarrier in % that was determined as follow [26]:

%DL=((total weight of drug-weight of drug in supernatant)/weight of nanocarrier)´100 (1)

Since, all of the initial loaded drug was transferred to dialysis bag to avoid from the wastage of 5FU, therefore, the entrapment efficacy percentage was not reported.

Drug release

For release study, the dialysis bags were separately immersed in 15 ml of PBS at pH 7.4 with a magnetic stirrer 100 rpm at 310 K. Furthermore, the immersion condition was contained by collecting 2 ml of release medium and replacing an equivalent amount of PBS on a regular basis. The percentage of cumulative drug release was determined as follow [27,28]:

$$\%\text{cumulative release} = C/C_0 \times 100$$

Where, C and C_0 are concentration of 5FU released from nanocarrier and total concentration of 5FU loaded nanocarrier, respectively. All experiments were performed triplicate and the averages and standard deviations were calculated.

Release mechanism

Zero-order ($M_t = M_0 + k_0\ t$), First-order ($\log M_t/M_0 = -k_1\ t/2.303$) and Korsmeyer-Peppas ($\log M_t/M_\infty = \log k_p + n \log t$) kinetic models were utilized to explore the release mechanism of drug from spherical nanocarriers [29–31], the highest R-squared (R^2) of models shows release mechanism follows from that kinetic model.

where M_t, M_0 and $M_¥$ are the concentration of drug dissolved in time, t, the initial amount of drug in the solution (most times, $M_0 = 0$), and the maximum of released drug, respectively, and k_0 is the zero-order release constant that obtained from slope of M_t versus t, k_1 is the first-order release constant that determined from slope of $\log M_t/M_0$ versus t, k_p is the Korsmeyer-Peppas release constant and n is the release exponent that calculated from slope and intercept of $\log M_t/M_\infty$ versus log t, respectively where M_t/M_∞ is lower than 0.6. The value of n can explain the type of release diffusion so that, $n < 0.43$ indicates a Fickian diffusion mechanism and $0.43<n<0.89$ shows a non-Fickian diffusion mechanism in spherical shape of particles [30].

Furthermore, the maximum amount of released drug (C_{max}), the kinetic constant of release (k_{rel}) and the initial release rate (r_0) were determined as following equation [32]:

$$t/C_t = \alpha + \beta t \quad (3)$$

where, C_t is the amount of released drug at time t, $\beta = 1/C_{max}$ is the inverse of C_{max}, $\alpha = 1/(C_{max})^2\ k_{rel}$ and $r_0 = 1/k_{rel}$ [10]. The intercept and slop of t/C_t versus t plot showed a and b, respectively.

MTT assay

Cell culture

Mouse 4T1 breast tumor cell lines were cultured in RPMI-1640 medium supplemented with 10% FBS and 1% penicillin–streptomycin antibiotic mixture at 310 K in a humidified incubator with 5% CO_2. The culture medium was changed every three days. When the cells reached the appropriate density, they were used for further analysis.

Cell viability

The cytotoxic evaluation of three systems of 5FU.Exo, 5FU@BSANP and 5FU.Exo@ BSANP (the concentration of 5FU, Exo and BSANP were 1.5 mg/ml, 24.3 mM and 4.67 mg/ml, respectively in all of the systems) was performed by MTT assay. For this purpose, the cultured medium (5×10^4 cells/well) was seeded for 24 h at 310 K with 90% humidity. After the incubation period, the medium was changed with a medium containing

5FU.Exo, 5FU@BSANP and 5FU.Exo@ BSANP for treatment cells during 24 h and concentration range of 5FU between 0-1.2 mM. Next, 10 mL of MTT solution (5 mg/mL) was added per well to the formed formazan crystal and incubated for 4 h at 310 K in darkness. To dissolve of formazan crystals, the above media were removed and 100 mL DMSO was added to each well. Finally, the absorbance of the supernatant solution was recorded at 570 nm by a microplate reader (Biotake, US) after 20 min. The cell viability percentage were calculated as follows [12]:

$$\% \text{ cell viability} = A_{treated}/A_{control} \times 100 \quad (4)$$

where $A_{treated}$ and $A_{control}$ were absorbance of the treated cells and untreated cells, respectively. All experiments were repeated in three times.

Statistical analysis

One-way ANOVA was used for examining the statistical significance of results with quantitative results reported as means ± standard deviations (SD) and Student's t-test (*$p < 0.05$; **$p<0.005$).

RESULTS AND DISCUSSION

Characterization

FTIR spectra of 5FU, Exo, BSANP, 5FU@ Exo, 5FU@BSANP and 5FU.Exo@BSANP were recorded (Fig. 1a) and the obtained results were summarized in Table. 1. FTIR spectrum of BSANP was compared with BSA powder and shown that absorption bands of BSA powder at 3372 cm^{-1} (amide A, N-O stretching), 2962 cm^{-1} (amide B, N-H stretching), 1655 cm^{-1} (amide I, C=O stretching), 1534 cm^{-1} (amide II, C-N stretching and N-H vibrating) and 932 cm^{-1} (amide III, C-N stretching and N-H bending) shifted to 3428 cm^{-1}, 2956 cm^{-1}, 1659 cm^{-1}, 1534 cm^{-1} and 946 cm^{-1} without any additional and removal of bands [33–35]. However, the peak positions of N-O and C=O have more changes due to formation of BSANP and binding to -N=C=N- groups of EDC crosslinker. The characteristic FTIR bands of 5FU were demonstrated at 3102 cm^{-1}, 1649 cm^{-1}, 1545 cm^{-1} and 1174 cm^{-1} that were attributed to N-H stretching of amide B, C=O stretching of amide I, N-H bending and C-F stretching mode, respectively. The spectra of 5FU.Exo and 5FU@ BSANP were shown that there were the main peak positions of all of them with chemical shift due to conjugation 5FU to Exo [36] and BSANP, separately. The remarkable point was significant shifts of -NH and -CO groups that indicated a possibility of binding in the two functional groups of samples. In addition, the absorption bands of 5FU.Exo@BSANP in comparison with 5FU, Exo and BSANP were shown their main bands with a shift in peak positions specially in amide B, amide I and C-F stretching due to the conjugation and the formation of 5FU.Exo@BSANP.

Comparison between FESEM images of BSANP, 5FU.Exo and 5FU.Exo@BSANP indicated that the shaped of BSANP was spherical while 5FU. Exo was rod shaped in 5FU.Exo@BSANP image. However, the size of 5FU.Exo was significantly lower than BSANP which is related to the loading of 5FU.Exo into the spherical BSANP as well as a colloidal formation, as shown in Fig. 1c without the obvious grain boundaries like BSANP. Further, the average size of the above systems was determined using Image J software which was found as 313±60 nm, 200±36 nm (width) and 403±64 for BSANP, 5FU.Exo and 5FU.Exo@BSANP, respectively. These results confirmed the loading of 5FU.Exo into BSANP and formation of 5FU.Exo@BSANP with no significant changes in shape and the enlargement of their average size in (approximately 90 nm) comparison to BSANP.

To further study the created structures, AFM analysis of BSANP, 5FU.Exo, and 5FU.Exo@BSANP was performed (Fig. 1 below) and the surface profile parameters [37,38] (Fig. S1b) demonstrated smooth roughness in 5FU@Exo.BSANP as compared with BSANP and 5FU.Exo, average roughness value (R_a) of 5FU.Exo@BSANP was 1.88 nm, while it was 3.63 nm and 4.02 nm for BSANP and 5FU. Exo, respectively. Subsequently, the formation of 5FU.Exo@BSANP caused reduction of roughness which is probably a satisfied system for biological applications due to smooth surface and prevention of damage to organs.

All of the obtained results of the above analysis confirmed the preparation of drug conjugated nanocarriers. Subsequently, another analysis was carried out for enhancement of efficacy and reduction of side effects.

Drug loading

Standard curve

As shown in Fig. 2a, a characteristic peak of 5FU was obtained at l_{max}=325 nm and selected for further studies. The standard curve was plotted (Fig. 2b) according to section 2.3.4 and the standard equation was obtained that was A=0.2206[C].

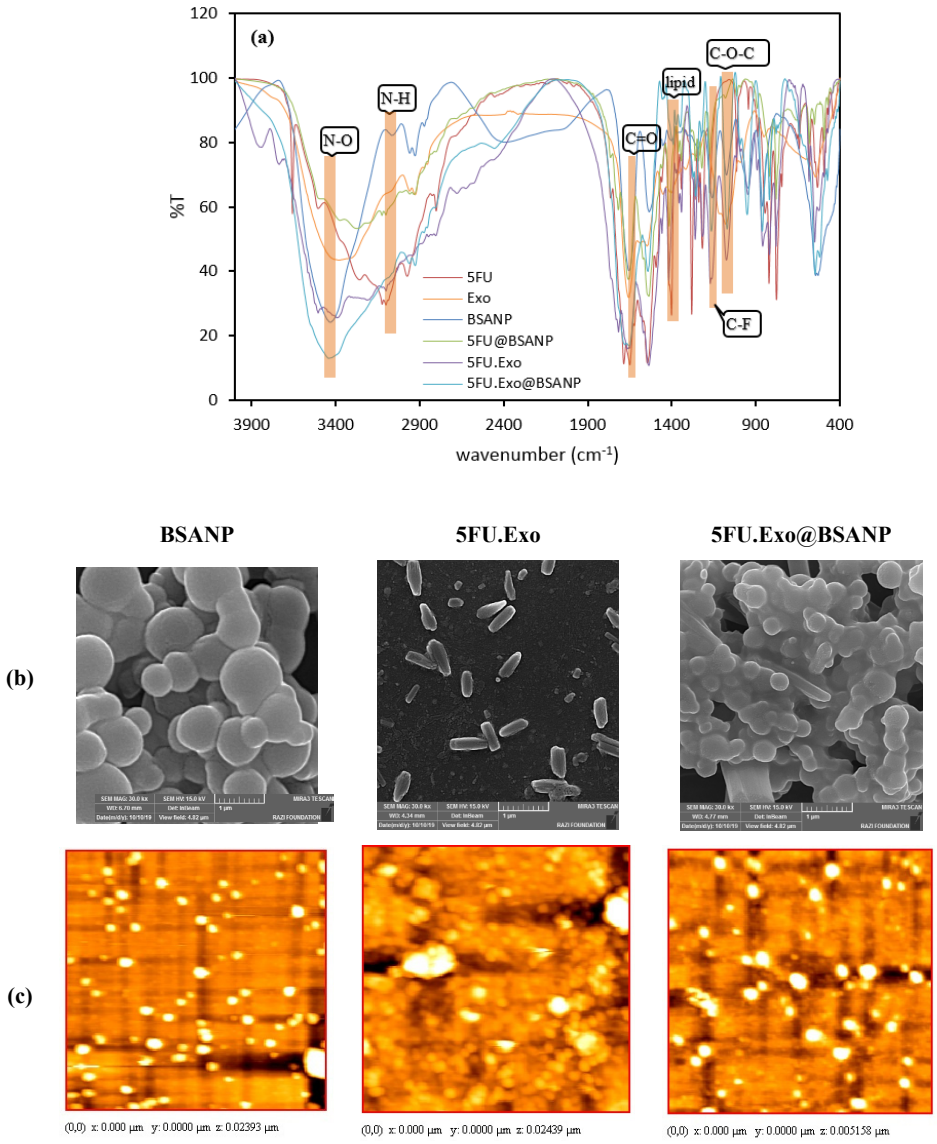

Fig. 1. FTIR (a), SEM (b) and AFM (c) images of BSANP, 5FU.Exo and 5FU.Exo@BSANP

Table 1. FTIR bands of samples

system	amide A, N-O stretching	amide B, N-H stretching	amide I, C=O stretching	amide II, C-N stretching and N-H vibrating	amide III, C-N stretching and N-H bending	C-F stretching	Lipid	C-O-C symmetric stretching
BSA powder	3372	2961	1655	1534	932	-	-	-
BSANP	3428	2956	1659	1534	946	-	-	-
5FU	-	3102	1649	1545	-	1174	-	-
Exo	-	2959	1660	1545	-	-	1454	1081
5FU.Exo	-	2943	1651	1535	-	1174	1459	1076
5FU@BSANP	3374	2937	1658	1537	892	1159	-	-
5FU.Exo@BSANP	3438	2932	1654	1542		1165	1391	1071

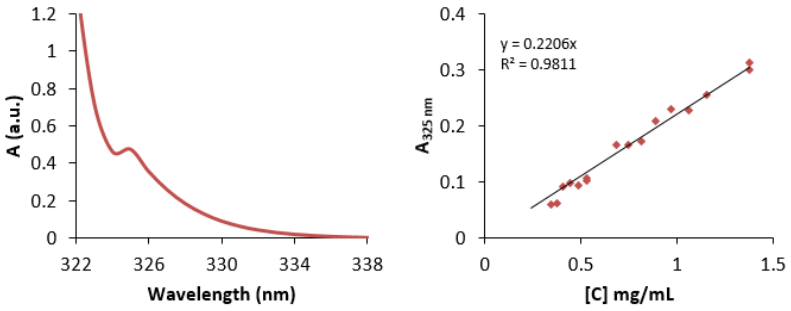

Fig. 2. The UV-Vis spectrum (a) and standard curve of 5FU (b)

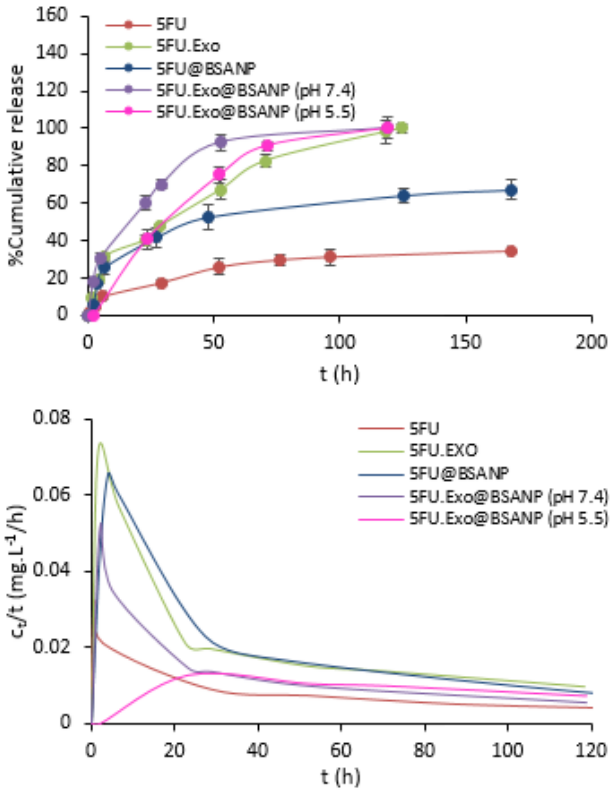

Fig. 3. Plots of cumulative drug release percentage (above) and release rate (bottom) versus time for only 5FU, 5FU@Exo, 5FU@BSANP, 5FU@Exo.BSANP at pH 7.4 and 5FU@Exo.BSANP at pH 5.5

Drug loading percentage

The percentage of drug loading of 5FU@BSANP and 5FU.Exo@ BSANP was determined according to Eq. 1 which was 63% and 31%, respectively. It was observed that the conjugation of 5FU to Exo reduced the loading of 5FU onto BSANP. In addition, 5FU and 5FU.Exo at their same concentration with the above systems were prepared for comparing the releasing behavior of drug from the carriers.

Drug release

The release of 5FU from Exo, BSANP, Exo@BSANP carriers was separately performed and compared with the release of only 5FU. All of the plots of cumulative drug release versus time of above systems were gathered in Fig. 3a. The behavior of 5FU demonstrated a sustained release of 35% during 168 h when it has no carrier. Also, the BSANP carrier caused sustained release of 5FU at the same time with 79% of release which may be due to enhanced

Table 2. The kinetic parameters of 5FU release from carriers

pH	Sample	Zero order	First order	Korsmeyer-peppas			Kinetic parameters		
		R^2	R^2	R^2	k_p	n	C_{max} (mg/ml)	k_r (ml/mg.h)	r_0 (mg.h/ml)
7.4	5FU	0.56	0.36	0.97	0.31	0.25	0.54	139.38	0.08
	5FU@Exo	0.92	0.80	0.94	0.33	0.22	1.55	9.38	0.11
	5FU@BSANP	0.74	0.49	0.88	0.36	0.20	1.23	14.08	0.07
	5FU@Exo.BSANP	0.85	0.66	0.99	0.40	0.20	0.76	47.43	0.02
5.5	5FU@Exo.BSANP	0.90	0.81	0.54	-	-	1.03	33.48	0.03

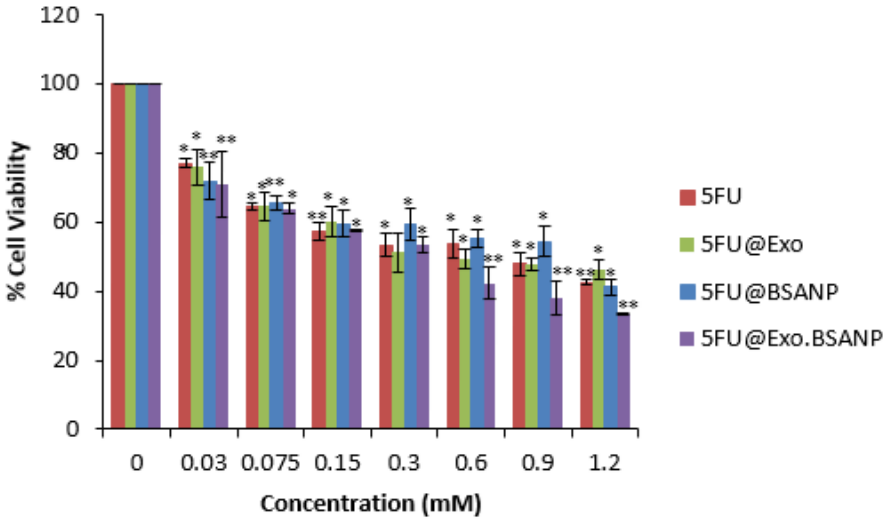

Fig. 4. MTT assay of 5FU, 5FU.Exo, 5FU@BSANP and 5FU.Exo@BSANPsystems onto 4T1 cell lines at 48 h and 0-1.2 mM concentration of drug. Values are the average of three separate experiments and are expressed as mean ± SD. *$p < 0.05$; **$p<0.005$.

stability of 5FU into BSANP and detection facility of drug. In contrast, release of drug from systems with exosome was faster, 5FU.Exo and 5FU@BSANP followed a complete release (100%) at 124 h, while the explosive release of 5FU from 5FU.Exo@BSANP was slower at pH 5.5 than 7.4 during that time. This is related to more acidic release media and reluctance of drug for entering it. Meanwhile, the release rate of the above systems is shown in Fig. 3b, revealing that the release rate of 5FU was significantly lower in acidic medium without increasing of rate in comparison with neutral medium. Thus, Exo@BSANP was the favorable system for release of 5FU at acid medium which can reduce the side effects of drug to normal cells during the treatment.

Furthermore, the other studies should be performed for efficacy of drug in nanocarriers. For this reason, the release mechanism and cytotoxicity of systems were carried out.

Release mechanism

The release of 5FU from various carriers was evaluated by three kinetic models. As reported in Table 2 and Fig. S2, the release mechanism best fitted (according to R^2 value) the Korsmeyer-Peppas kinetic model at pH 7.4 which can be described the type of diffusion, the value of "n" lower than 0.43 indicated that the diffusion mechanism followed by Fickian. However, the release mechanism of 5FU@Exo.BSANP system followed zero order model at pH 5.5.

Further, the other kinetic parameters (Table 2 and Fig. S3) were also shown the maximum concentration of released drug (C_{max}) increased in the presence of carriers. In addition, the initial release rate of 5FU@Exo.BSANP was lower than in other systems confirming the obtained results of Fig. 3b and showing that the presence of Exo and BSANP reduced the initial release of 5FU up to twice as compared to the other carriers. Subsequently, the designed carriers help the sustained release of 5FU with elevation of released drug concentration and reduction of release rate. However, the function of 5FU@Exo.BSANP was better in acidic medium and

it is an appropriate candidate for local injection.

MTT assay

In vitro studies of 5FU, 5FU.Exo, 5FU@BSANP and 5FU.Exo@BSANP were performed onto breast cancer cell lines, 4T1 by MTT assay. As depicted in Fig. 4, the cell viability percentage was reduced with elevation of the concentration of samples showing they were dose-dependent. Further, the cancer cell death of 5FU.Exo@BSANP (33.31%±0.075 in 1.2 mM) was higher than only drug (42.40%±0.71 in 1.2 mM). Also, each of the carriers alone (5FU.Exo, 5FU@BSANP) did not have the required efficiency for the death of 4T1 cancer cells; in the 50% cytotoxic concentration (CC50) of 5FU.Exo@BSANP (0.3 mM), this value was 0.9 mM, 0.6 mM and 0.9 mM for 5FU, 5FU.Exo, 5FU@BSANP, respectively.

CONCLUSION

A new biocompatible nanocarrier based on BSA and Exo conjugated with 5FU as an anticancer drug (5FU.Exo@BSANP) was prepared and characterized by FTIR, AFM and FESEM. The results confirmed 5FU.Exo@BSANP formation. Then, drug release profiles and the mechanism of the above-mentioned system was analyzed through UV-Vis spectroscopy and compared to 5FU.Exo and 5FU@BSANP. The obtained results indicated that the release of 5FU from 5FU.Exo@BSANP was more sustained than in the other systems. Thus, the designed system improved the life time of drug in the body. To evaluate the cell viability of systems, MTT assay was performed onto 4T1 cancer cell line that showing more cytotoxicity of 5FU.Exo@BSANP. These notable achievements introduce a nanocarrier with the capacity of sustained release of drug with enhancing its effectiveness.

ACKNOWLEDGMENTS

The authors are grateful for the financial support with research grant (no. 771398054) from the Materials and Energy Research Center (MERC), Karaj, Iran.

CONFLICT

The authors have no conflict of interest.

REFERENCES

1. Eskandari S, Barzegar A, Mahnam K. Absorption of daunorubicin and etoposide drugs by hydroxylated and carboxylated carbon nanotube for drug delivery: theoretical and experimental studies. Journal of Biomolecular Structure and Dynamics. 2021:1-8.
2. R. Duan, L. Wang, W. Huo, S. Chen, X. Zhou, Spectrochimica Acta Part A : Molecular and Biomolecular Spectroscopy Synthesis , crystal structures , DNA binding and photoluminescence properties of [Cu (pzta) 2 Cl] Cl Á H 2 O for DNA detection, Spectrochim. ACTA PART A Mol. Biomol. Spectrosc. 128 (2014) 614–621. https://doi.org/10.1016/j.saa.2014.02.111.
3. Izadiyan Z, Shameli K, Teow S-Y, Yusefi M, Kia P, Rasouli E, et al. Anticancer Activity of 5-Fluorouracil-Loaded Nanoemulsions Containing Fe3O4/Au Core-Shell Nanoparticles. Journal of Molecular Structure. 2021;1245:131075.
4. Zwain T, Taneja N, Zwayen S, Shidhaye A, Palshetkar A, Singh KK. Albumin nanoparticles—A versatile and a safe platform for drug delivery applications. Nanoparticle Therapeutics: Elsevier; 2022. p. 327-58.
5. Raghav N, Sharma MR. Usage of nanocrystalline cellulose phosphate as novel sustained release system for anti-inflammatory drugs. Journal of Molecular Structure. 2021;1233:130108.
6. Kavousi F, Goodarzi M, Ghanbari D, Hedayati K. Synthesis and characterization of a magnetic polymer nanocomposite for the release of metoprolol and aspirin. Journal of Molecular Structure. 2019;1183:324-30.
7. Bicak B, Budama-Kilinc Y, Kecel-Gunduz S, Zorlud T, Akman G. Peptide based nano-drug candidate for cancer treatment: Preparation, characterization, in vitro and in silico evaluation. Journal of Molecular Structure. 2021;1240:130573.
8. Tian X, Yang N, Sun M, Li Y, Wang W. Preparation, physicochemical, and antibacterial properties of bovine serum albumin microspheres loaded with sodium nitrite. LWT. 2022;154:112835.
9. Solanki R, Patel K, Patel S. Bovine Serum Albumin Nanoparticles for the Efficient Delivery of Berberine: Preparation, Characterization and In vitro biological studies. Colloids and Surfaces A: Physicochemical and Engineering Aspects. 2021;608:125501.
10. Shahlaei M, Saeidifar M, Zamanian A. Increasing the effectiveness of oxaliplatin using colloidal immunoglobulin G nanoparticles: Synthesis, cytotoxicity, interaction, and release studies. Colloids and Surfaces B: Biointerfaces. 2020;195:111255.
11. Solanki R, Rostamabadi H, Patel S, Jafari SM. Anticancer nano-delivery systems based on bovine serum albumin nanoparticles: A critical review. International Journal of Biological Macromolecules. 2021;193:528-40.
12. Prabha G, Raj V. Sodium alginate–polyvinyl alcohol–bovin serum albumin coated Fe3O4 nanoparticles as anticancer drug delivery vehicle: Doxorubicin loading and in vitro release study and cytotoxicity to HepG2 and L02 cells. Materials Science and Engineering: C. 2017;79:410-22.
13. Chinnappan M, Srivastava A, Amreddy N, Razaq M, Pareek V, Ahmed R, et al. Exosomes as drug delivery vehicle and contributor of resistance to anticancer drugs. Cancer Lett. 2020;486:18-28.
14. Patil SM, Sawant SS, Kunda NK. Exosomes as drug delivery systems: A brief overview and progress update. European Journal of Pharmaceutics and Biopharmaceutics. 2020;154:259-69.
15. Zhang Y, Bi J, Huang J, Tang Y, Du S, Li P. Exosome: A Review of Its Classification, Isolation Techniques, Storage, Diagnostic and Targeted Therapy Applications. Int J Nanomedicine. 2020;15:6917-34.

16. Yu Y, Zhang WS, Guo Y, Peng H, Zhu M, Miao D, et al. Engineering of exosome-triggered enzyme-powered DNA motors for highly sensitive fluorescence detection of tumor-derived exosomes. Biosensors and Bioelectronics. 2020;167:112482.
17. Liu J, Ren L, Li S, Li W, Zheng X, Yang Y, et al. The biology, function, and applications of exosomes in cancer. Acta Pharm Sin B. 2021;11(9):2783-97.
18. Jiang X-C, Gao J-Q. Exosomes as novel bio-carriers for gene and drug delivery. International Journal of Pharmaceutics. 2017;521(1-2):167-75.
19. Sheller-Miller S, Menon R. Isolation and characterization of human amniotic fluid-derived exosomes. Methods in Enzymology: Elsevier; 2020. p. 181-94.
20. Bhusnure OG, Gholve SB, Giram PS, Gaikwad AV, Udumansha U, Mani G, et al. Novel 5-flurouracil-Embedded non-woven PVA - PVP electrospun nanofibers with enhanced anti-cancer efficacy: Formulation, evaluation and in vitro anti-cancer activity. Journal of Drug Delivery Science and Technology. 2021;64:102654.
21. Shehatta NH, Okda TM, Omran GA, Abd-Alhaseeb MM. Baicalin; a promising chemopreventive agent, enhances the antitumor effect of 5-FU against breast cancer and inhibits tumor growth and angiogenesis in Ehrlich solid tumor. Biomedicine & Pharmacotherapy. 2022;146:112599.
22. Adhikari P, Pal P, Das AK, Ray S, Bhattacharjee A, Mazumder B. Nano lipid-drug conjugate: An integrated review. International Journal of Pharmaceutics. 2017;529(1-2):629-41.
23. Jalalvandi E, Hanton LR, Moratti SC. Preparation of a pH sensitive hydrogel based on dextran and polyhydrazide for release of 5-flurouracil, an anticancer drug. Journal of Drug Delivery Science and Technology. 2018;44:146-52.
24. Ziaaddini V, Saeidifar M, Eslami-Moghadam M, Saberi M, Mozafari M. Improvement of efficacy and decrement cytotoxicity of oxaliplatin anticancer drug using bovine serum albumin nanoparticles: synthesis, characterisation and release behaviour. IET Nanobiotechnol. 2020;14(1):105-11.
25. Rezk AI, Obiweluozor FO, Choukrani G, Park CH, Kim CS. Drug release and kinetic models of anticancer drug (BTZ) from a pH-responsive alginate polydopamine hydrogel: Towards cancer chemotherapy. International Journal of Biological Macromolecules. 2019;141:388-400.
26. V.F. Lotfy, A.H. Basta, Jo ur, Int. J. Biol. Macromol. (2020). https://doi.org/10.1016/j.ijbiomac.2020.10.047.
27. Pooresmaeil M, Javanbakht S, Behzadi Nia S, Namazi H. Carboxymethyl cellulose/mesoporous magnetic graphene oxide as a safe and sustained ibuprofen delivery bio-system: Synthesis, characterization, and study of drug release kinetic. Colloids and Surfaces A: Physicochemical and Engineering Aspects. 2020;594:124662.
28. Li C, Fang K, He W, Li K, Jiang Y, Li J. Evaluation of chitosan-ferulic acid microcapsules for sustained drug delivery: Synthesis, characterizations, and release kinetics in vitro. Journal of Molecular Structure. 2021;1227:129353.
29. Main mechanisms to control the drug release 4, (2015). https://doi.org/10.1016/B978-0-08-100092-2.00004-7.
30. Mathematical models of drug release 5, (2015). https://doi.org/10.1016/B978-0-08-100092-2.00005-9.
31. G. Arora, K. Malik, Formulation and Evaluation of Mucoadhesive Matrix Tablets of Taro Gum : Optimization Using Response Surface Methodology Formułowanie i ocena mukoadhezyjnych matryc tabletek gumy Taro : optymalizacja wyników przy zastosowaniu metody powierzchni odpowiedzi, 30 (2011).
32. Singh B, Singh B. Influence of graphene-oxide nanosheets impregnation on properties of sterculia gum-polyacrylamide hydrogel formed by radiation induced polymerization. International Journal of Biological Macromolecules. 2017;99:699-712.
33. Retnakumari A, Setua S, Menon D, Ravindran P, Muhammed H, Pradeep T, et al. Molecular-receptor-specific, non-toxic, near-infrared-emitting Au cluster-protein nanoconjugates for targeted cancer imaging. Nanotechnology. 2009;21(5):055103.
34. Emadi F, Amini A, Gholami A, Ghasemi Y. Functionalized Graphene Oxide with Chitosan for Protein Nanocarriers to Protect against Enzymatic Cleavage and Retain Collagenase Activity. Sci Rep. 2017;7:42258-.
35. Ziaaddini V, Saeidifar M, Eslami-Moghadam M, Saberi M, Mozafari M. Improvement of efficacy and decrement cytotoxicity of oxaliplatin anticancer drug using bovine serum albumin nanoparticles: synthesis, characterisation and release behaviour. IET Nanobiotechnol. 2020;14(1):105-11.
36. Soares Martins T, Magalhães S, Rosa IM, Vogelgsang J, Wiltfang J, Delgadillo I, et al. Potential of FTIR Spectroscopy Applied to Exosomes for Alzheimer's Disease Discrimination: A Pilot Study. Journal of Alzheimer's Disease. 2020;74(1):391-405.
37. R.R.L. De Oliveira, D.A.C. Albuquerque, T.G.S. Cruz, Measurement of the Nanoscale Roughness by Atomic Force Microscopy : Basic Principles and Applications, (n.d.).
38. M. Raposo, Q. Ferreira, P.A. Ribeiro, A Guide for Atomic Force Microscopy Analysis of Soft- Condensed Matter, (2007) 758–769.